Published in final edited form as:
J Speech Lang Hear Res. 2009 August ; 52(4): 1008–1020. doi:10.1044/1092-4388(2009/08-0049).

A Rat Excised Larynx Model of Vocal Fold Scar

Nathan V. Welham, Ph.D.[1], **Douglas W. Montequin, Ph.D.**[2], **Ichiro Tateya, M.D., Ph.D.**[3], **Tomoko Tateya, M.D., Ph.D.**[3], **Seong Hee Choi, Ph.D.**[1], and **Diane M. Bless, Ph.D.**[1]

[1]Division of Otolaryngology-Head and Neck Surgery, Department of Surgery, University of Wisconsin School of Medicine and Public Health, Madison, Wisconsin

[2]The National Center for Voice and Speech, The Denver Center for the Performing Arts, Denver, Colorado

[3]Department of Otolaryngology-Head and Neck Surgery, Graduate School of Medicine, Kyoto University, Kyoto, Japan

Abstract

Purpose—To develop and evaluate a rat excised larynx model for the measurement of acoustic, aerodynamic and vocal fold vibratory changes resulting from vocal fold scar.

Method—Twenty four 4-month-old male Sprague Dawley rats were assigned to one of four experimental groups: Chronic vocal fold scar, chronic vocal fold scar treated with 100 ng basic fibroblast growth factor (bFGF), chronic vocal fold scar treated with saline (sham treatment), and unscarred untreated control. Following tissue harvest, histological and immunohistochemical data were collected to confirm extracellular matrix alteration in the chronic scar group, and acoustic, aerodynamic and high speed digital imaging data were collected using an excised larynx setup in all groups. Phonation threshold pressure (P_{th}), glottal resistance (R_g), glottal efficiency (E_g), vibratory amplitude and vibratory area were employed as dependent variables.

Results—Chronically scarred vocal folds were characterized by elevated collagen I and III and reduced hyaluronic acid abundance. Phonation was achieved and data were collected from all control and bFGF treated larynges, however phonation was not achieved with 3 of 6 chronically scarred and 1 of 6 saline treated larynges. Compared to control, the chronic scar group was characterized by elevated P_{th}, reduced E_g, and intra-larynx vibratory amplitude and area asymmetry. The bFGF group was characterized by P_{th} below control group levels, E_g comparable to control, and vocal fold vibratory amplitude and area symmetry comparable to control. The sham group was characterized by P_{th} comparable to control, E_g superior to control, and vocal fold vibratory amplitude and area symmetry comparable to control.

Conclusions—The excised larynx model reported here demonstrated robust deterioration across phonatory indices under the scar condition and sensitivity to treatment induced change under the bFGF condition. The improvement observed under the sham condition may reflect unanticipated therapeutic benefit or artifact. This model holds promise as a tool for the functional characterization of biomechanical tissue changes resulting from vocal fold ECM injury, and the evaluation of experimental therapies.

Correspondence: Nathan V. Welham, Ph.D., K4/723 CSC, 600 Highland Avenue, Madison WI, 53792, USA.

This paper will be published in its final form in the *Journal of Speech, Language, and Hearing Research*, accessible online at http://jslhr.asha.org/

Keywords

Rat excised larynx; vocal fold scar; basic fibroblast growth factor; subglottal pressure; glottal resistance; glottal efficiency; high speed digital imaging

Introduction

Vocal fold scar results from abberant extracellular matrix (ECM) remodeling following injury (Rousseau et al., 2003; Tateya, Tateya, Sohn, & Bless, 2005; Thibeault, Gray, Bless, Chan, & Ford, 2002) and is typically associated with poor vocal fold oscillation during phonation (Hirano, Bless, Nagai et al., 2004; Rousseau, Montequin, Tateya, & Bless, 2004). Dysphonia secondary to vocal fold scar presents a significant clinical challenge, and an emerging body of literature is focused on the characterization and treatment of this recalcitrant condition. A number of promising treatment approaches have been reported, involving cell delivery (Chhetri et al., 2004; Hertegard et al., 2006; Kanemaru et al., 2003; Krishna, Rosen, Branski, Wells, & Hebda, 2006), various scaffolds and biomaterials (Duflo, Thibeault, Li, Shu, & Prestwich, 2006; Hansen, Thibeault, Walsh, Shu, & Prestwich, 2005; Jia et al., 2006; Xu, Chan, & Tirunagari, 2007), and growth factor, phytochemical and pharmacological agents (Hirano, Bless, Nagai et al., 2004; Hirano, Bless, Rousseau et al., 2004; Luo, Kobler, Zeitels, & Langer, 2006; Ohno et al., 2007; Rousseau, Tateya, Lim, Muñoz del Río, & Bless, 2006).

The evaluation of experimental treatments for vocal fold scar is generally based on cellular and extracellular assays, such as the measurement of inflammatory mediators produced by resident and invading cell populations, transcription and translation levels of key ECM genes and proteins, and protein organization within the ECM; in addition to biomechanical tissue assays, such as those offered by rheological measurements of tissue viscoelasticity, and physiological measurements of vocal fold vibratory function during *in vivo* or *ex vivo* phonation. Given that the dysphonia resulting from vocal fold scar is a fundamentally biomechanical problem, these functional assays are critical when assessing the outcome of any scar related experimental manipulation. Rheologic and phonatory data have been reported in canine, porcine and rabbit models (Hirano, Bless, Nagai et al., 2004; Hirano, Bless, Rousseau et al., 2004; Rousseau, Hirano et al., 2004; Rousseau et al., 2003; Rousseau, Montequin et al., 2004; Rousseau et al., 2006; Thibeault et al., 2002), but with the exception of one paper presenting dynamic spring rate from a single larynx (Dailey, Tateya, Montequin, Welham, & Goodyer, in press), have not been reported in the rat; presumably due to the technical challenge of generating valid and reliable data from such a small larynx.

Rat Experimental Models

Rat experimental models are ubiquitous in biomedical research and hold several distinct advantages for vocal fold scar research. First, the rat vocal fold lamina propria contains a tri-layered structure which is similar in morphology and fibrous protein composition to humans (Kurita, Nagata, & Hirano, 1983). Second, rat genome sequence data are readily available (Petersen et al., 2005), which affords the use of computational biology techniques for mining large transcriptomic and proteomic datasets. Third, the formation of chronic vocal fold scar has been reported two months following injury in the rat (Tateya et al., 2005), but may take as long as six months in the canine and rabbit (Rousseau, Hirano et al., 2004; Rousseau et al., 2003).

It is likely, however, that the rat larynx has different biomechanical and phonatory properties than are seen in larger animals and humans; based on its comparative anatomy. Kurita et al. (1983) reported that the rat membranous vocal fold has an average length of 1 mm and

average mucosal thickness of 0.2 mm; yielding a length-to-thickness ratio of 5:1. In contrast, they reported an average length of 15 mm and average thickness of 3 mm (ratio 5:1) in the canine, and a length of 15 mm and thickness of 1.1 mm (ratio 14:1) in a single adult male human control. As membranous vocal fold length and mucosal thickness are fundamental anatomical variables that are known to influence phonatory output (Chan & Titze, 2006; Lucero & Koenig, 2005; Titze, 1988, 1989), these differences are undoubtedly important to the interpretation and generalization of excised larynx phonation data from the rat.

Excised Larynx Phonation

Excised larynx models have been used in the modern study of vocal fold physiology for approximately 50 years (van den Berg, 1960; van den Berg & Tan, 1959). Although devoid of innervation and active muscle control, excised larynx set-ups allow the systematic manipulation of glottal configuration and directional tension forces, air temperature and humidity, and subglottal pressure (P_s) and flow (U). In addition, excised larynx approaches allow the straightforward collection of data that are either challenging or impossible to obtain using human and animal *in vivo* set-ups, such as the measurement of glottal source parameters without the influence of the vocal tract, the measurement of vocal fold impact stress, and the examination of vocal fold vibration from an inferior or medial (i.e., using a hemilarynx) observation position. Recent work in this area has focused on medial surface dynamics during vocal fold vibration (Döllinger & Berry, 2006a, 2006b), non-linear pressure-flow and pressure-frequency relationships (Alipour & Jaiswal, in press; Alipour & Scherer, 2007), non-linear vibratory patterns present at high P_s (Jiang, Zhang, & Ford, 2003; Jiang, Zhang, & Stern, 2001; Zhang, Jiang, Tao, Bieging, & MacCallum, 2007), flow velocity fields and flow vortices (Khosla, Murugappan, Gutmark, & Scherer, 2007; Khosla, Murugappan, Lakhamraju, & Gutmark, 2008), and the influence of supraglottic anatomy on phonation (Alipour, Jaiswal, & Finnegan, 2007; Döllinger, Berry, & Montequin, 2006; Finnegan & Alipour, in press).

A number of phonation indices, measureable using an excised larynx system, are potentially sensitive to the viscoelastic tissue changes typically seen in the scarred vocal fold. Phonation threshold pressure (P_{th}), defined as the minimum P_s required to initiate self-sustained vocal fold oscillation, has been shown to vary proportionally alongside changes in vocal fold tissue viscosity in theoretical, computational and physical models (Berry, Reininger, Alipour, Bless, & Ford, 2005; Chan & Titze, 2006; Titze, 1988); as well as in porcine and rabbit excised larynx studies of vocal fold scar (Hirano, Bless, Rousseau et al., 2004; Rousseau, Montequin et al., 2004; Rousseau et al., 2006). Glottal efficiency (E_g), defined as the ratio of radiated acoustic power to aerodynamic input power, may be negatively affected by elevated vocal fold tissue viscosity due to increased power consumption/loss at the level of the vocal folds (Titze, 1988). Glottal resistance (R_g), defined as the ratio of transglottal pressure to transglottal flow, may be elevated if increased P_s is required to drive vocal fold oscillation to achieve a target U. Finally, vocal fold vibratory parameters such as vibratory amplitude, vibratory area and mucosal wave excursion are known to be compromised in the presence of vocal fold scar (Benninger et al., 1996; Hirano, Rousseau et al., 2004). We employed these aerodynamic, acoustic and vibratory indices as dependant variables in this study based on their ability to characterize changes in vocal fold function secondary to altered viscoelasticity.

Basic Fibroblast Growth Factor

Basic fibroblast growth factor (bFGF), also referred to as FGF-2, is one of 22 known members of the vertebrate FGF superfamily (Ornitz & Itoh, 2001). It is expressed by a wide array of cell types, including fibroblasts, epithelial cells, endothelial cells, mast cells, megakaryocytes and platelets; and activates cell surface FGF receptors in conjunction with

heparan sulfate (Rapraeger, Krufka, & Olwin, 1991; Yayon, Klagsbrun, Esko, Leder, & Ornitz, 1991). bFGF promotes angiogenesis, is a potent mitogen, and was first named for its ability to induce fibroblast proliferation (Gospodarowicz, 1974, 1975). It has been shown to downregulate collagen I and tropoelastin mRNA transcription in periodontal ligament fibroblasts (Palmon et al., 2000, 2001), and upregulate hyaluronic acid (HA) synthesis in skin fibroblasts *in vitro* (Heldin, Laurent, & Heldin, 1989). bFGF has also been shown to potentiate leukocyte recruitment to inflammation sites in skin (Zittermann & Issekutz, 2006a, 2006b), and improve dermal wound healing outcomes when delivered using either direct injection (Ono et al., 2007), a targeted peptide delivery system (Zhao et al., in press), or alongside a tissue engineering scaffold (Akita, Akino, Tanaka, Anraku, & Hirano, 2008).

A series of studies have examined the effects of bFGF administration on vocal folds and vocal fold fibroblasts (VFFs) in culture. Hirano, Bless, Heisey, & Ford (2003) observed increased cell proliferation and HA synthesis (with no correlation between these variables) in canine VFFs across a 7 day period in response to either single or serial administration of 20 ng/mL bFGF. In a subsequent study, Hirano, Bless, Muñoz del Río, Connor, & Ford (2004) observed increased HA synthesis alongside decreased collagen I synthesis in young and old rat VFFs treated with either 20 or 200 ng/mL bFGF, irrespective of age condition or growth factor concentration. Luo et al. (2006), studying human VFFs in a three-dimensional hydrogel culture system, demonstrated increased cell proliferation, no change in HA and elastin synthesis, and decreased collagen and sulfated glycosaminoglycan synthesis following serial administration of 20 ng/mL bFGF over a 3 week period. Finally, using an *in vivo* aged rat model, Hirano et al. (2005) found increased HA but no change in collagen abundance, 2 months following the administration of 4 weekly 100 ng bFGF injections into the vocal fold.

We elected to include a bFGF experimental condition in this study as means to evaluate the sensitivity of our excised larynx set-up to therapeutic change, in contrast to the negative phonatory change expected with chronic vocal fold scar. As the scarred vocal fold is classically characterized by increased collagen and decreased HA abundance (Rousseau et al., 2003; Tateya et al., 2005), and bFGF has been shown to favorably modulate the abundance of these molecules as reported above, we anticipated a positive tissue response to bFGF administration in the scarred vocal fold.

Hypotheses

The purpose of this study was to determine if our excised larynx setup was sufficiently sensitive to scar and treatment induced biomechanical differences in laryngeal structures as small as those in the rat. We collected data from unscarred and chronically scarred larynges, in addition to chronically scarred larynges treated with a sham (saline) injection and therapeutic bFGF injection. ECM changes consistent with scar were confirmed in the chronically scarred larynges using histology and immunohistochemistry (IHC). We hypothesized that the chronically scarred and sham treated larynges would be characterized by elevated P_{th}, reduced E_g, elevated R_g, and reduced vibratory amplitude and area compared with control. We also hypothesized that the bFGF treated larynges would be characterized by reduced P_{th}, elevated E_g, reduced R_g, and improved vibratory amplitude and area compared with the untreated chronically scarred larynges.

Materials and Methods

Experimental Animal Procedures

Twenty four 4-month-old male Sprague Dawley rats were used in this study and assigned to chronic scar, bFGF treated, sham (saline) treated, and control groups. Eight rats underwent

unilateral vocal fold stripping with laryngeal harvest 2 months post injury (chronic scar group). Four rats underwent unilateral vocal fold stripping, injection of bFGF 2 months post injury, and laryngeal harvest 4 months post injury (bFGF treated group). Six rats underwent unilateral vocal fold stripping, injection of saline 2 months post injury, and laryngeal harvest 4 months post injury (sham treated group). Six rats underwent no vocal fold stripping or injection (control group).

Vocal fold injuries were created as previously reported (Tateya et al., 2005). Rats underwent anesthesia induction with isoflurane (2–3% delivered at 0.8–1.5 L/min) followed by maintenance using an intraperitoneal (IP) injection of ketamine hydrochloride (90 mg/kg) and xylazine hydrochloride (9 mg/kg). Atropine sulfate (0.05 mg/kg) was also injected IP to reduce the secretion of saliva and sputum in the laryngeal lumen. The animals were placed on an operating platform in a near-vertical position and a custom fabricated 1 mm diameter steel wire laryngoscope was inserted to facilitate vocal fold visualization. Vocal fold monitoring was performed using a 1.9 mm diameter 25° endoscope (Richard Wolf, Vernon Hills, IL) connected to an external light source and video monitor. Injuries were created by vocal fold stripping using a 25 G needle and microforceps.

Vocal fold injections were performed using a 50 μL, 50 mm, 26-gauge needle, under endoscopic guidance as described above. bFGF (Sigma-Aldrich, St. Louis, MO) was injected at a concentration of 100 ng in 10 μL; a 100 ng dose was selected based on Hirano et al. (2005). Normal saline (0.9% w/v NaCl) was injected in a volume of 10 μL.

Euthanasia was performed via intracardiac injection of Beuthanasia (0.22 mg/kg) (Schering-Plough Animal Health, Union, NJ). Larynges were harvested en bloc (Figure 1), quick frozen using liquid nitrogen, and stored at −80°C until use. Larynges from the chronic scar group intended for histological processing were embedded in optimal cutting temperature compound (Tissue-Tek, Sakura, Tokyo, Japan) prior to quick freezing.

Histology and Immunohistochemistry

Two chronically scarred larynges were reserved for histology and IHC to confirm ECM alteration 2 months following injury creation. Ten-μm coronal frozen sections were prepared using a cryostat (Leica, Wetzlar, Germany) and sections containing the mid-membranous vocal folds were employed for analysis. Masson's trichrome stain was used to detect collagen and Alcian blue stain (pH 2.5) was used to detect HA. A hyaluronidase digestion procedure was used to confirm the presence of HA (as opposed to other glycosaminoglycans) on Alcian blue stained sections. Alternate sections were incubated with 0.5 mg/mL bovine testicular hyaluronidase (Sigma-Aldrich, St. Louis, MO) for 1 hr at 37°C and HA abundance was evaluated by comparing digested with non-digested sections. Images were captured using a Nikon Eclipse E600 microscope (Nikon, Mellville, NY) and Pixera color digital camera (model PVC100C, Los Gatos, CA).

Fluorescent IHC was utilized to detect collagen type I and III. Sections were washed twice with phosphate buffered saline (PBS), fixed in 4% paraformaldehyde for 1 min at room temperature (RT), and again washed twice in PBS. Following blocking for 1 hr at RT, sections were incubated in primary antibody solution overnight at RT. Next, samples were washed and incubated for 1 hr at RT with the secondary antibody and 200 nmol/L TOTO-3 nuclear dye (Molecular Probes, Eugene, Oregon). Finally, samples were washed three times in PBS and coverslips were placed using Vectashield mounting medium (Vector Labs, Burlingame, CA). Images were captured using a laser scanning confocal microscope (Bio-Rad MRC-1024, Hercules, CA). Rat skin was used as a positive control. Omission of the primary antibody served as a negative control.

The primary antibodies used in this experiment were biotin conjugated goat anti-type 1 collagen (Southern Biotech, Birmingham, AL) at 1:50 dilution and rabbit anti-collagen type III (Rockland Immunochemicals, Gilbertsville, PA) at 1:100 dilution. The secondary antibodies used were fluorescein isothiocyanate-avidin D (Vector Labs, Burlingame, CA) at 1:1,000 dilution and Texas-Red conjugated anti-rabbit immunoglobulin G (Jackson Immunoresearch, West Grove, PA) at 1:400 dilution. Primary and secondary antibodies were diluted in 1% bovine serum albumin (BSA) and 0.1% Triton-X in PBS. Blocking was performed using 5% BSA and 0.1% Triton-X in PBS.

Two scarred and two control images were captured per stain/immunostain from each animal and all images were evaluated using consensus judgment performed by a panel of three judges. Scarred and control images from the same section were randomly assigned to right and left positions, image reflected where necessary, and arranged in conventional coronal orientation with both vocal folds facing a central lumen. Judges were instructed to identify whether the two vocal folds demonstrated equivalent stain/immunostain abundance, and if not, which vocal fold demonstrated greater abundance. Judgments were performed twice for each image pair, in a random sequence.

Excised Larynx Setup

Figure 2 and Figure 3 illustrate the excised larynx setup used in this experiment. The larynx was mounted on an inverted polypropylene pipette tip cut to match the diameter of the trachea. Pressurized air was warmed and humidified using a humidifier controller (3M, St. Paul, MN) and delivered to the trachea via a polyvinyl chloride tubing system. P_s was monitored using a U-tube manometer (Dwyer Instruments, Michigan City, IN) and data were collected using a Honeywell PK8772-4 microswitch pressure transducer (Honeywell, Morristown, NJ). U was monitored using a flowmeter (Gilmont Instruments, Barrington, IL) and data were collected using a Fleisch pneumotachograph combined with a Validyne DP-103 pressure transducer (Validyne, Northridge, CA). Acoustic data were collected using an omnidirectional dynamic microphone (Omnidyne 578, Shure, Niles, IL) placed at 45°, 15 cm from the glottis and connected to a Presonus Bluetube preamplifier (Presonus, Baton Rouge, LA). Acoustic intensity was monitored using a digital sound level meter (Radioshack, Fort Worth, TX), also placed at 45°, 15 cm from the glottis.

High-speed digital images (HSDI) of vocal fold vibration were captured at 13,500 fps using a Kodak Ektapro HS Motion Analyzer 4540 (Eastman Kodak, Rochester, NY) positioned superior to the glottis and controlled by a computer using a GPIB instrument controller card and IMAQ image acquisition card (National Instruments, Austin, TX). A 10 X microscope lens array (Leica Microsystems, Wetzlar, Germany) was mounted to the camera and used to magnify the glottis.

Aerodynamic, acoustic and HSDI trigger signals were digitized at 30 kHz using a second computer with a Dataq DI-720 analog-digital converter and WinDaq 2.72 data acquisition software (Dataq Instruments, Akron, OH).

Excised Larynx Experimental Protocol

Larynges were thawed at 4°C overnight, and the epiglottis, aryepiglottic folds and false vocal folds were removed to maximize exposure of the true vocal folds. Arytenoid adduction procedures were performed under magnification on each larynx using 8-0 Prolene sutures (Ethicon, Somerville, NJ). Following instrument calibration, each larynx was mounted and then subjected to gradual increases in P_s to obtain P_{th}. Aerodynamic, acoustic and vibratory data were then collected at 0.196 kPa (2 cm H_20) intervals from P_{th} to 5.884 kPa (60 cm H_20). Corresponding mean flow range was 0.033–0.075 L/s.

Data Analysis

All experimental data were analyzed using custom routines within MATLAB 6.1 (Mathworks, Natick, MA). E_g was calculated by dividing radiated acoustic power by mean aerodynamic power and converting to a percentage. Radiated acoustic power (in W) was converted from acoustic intensity in dB SPL, based on an assumption of uniform acoustic radiation from the glottis in all directions, and a spherical area of 0.28 m^2 at 15 cm from the glottis (distance to the sound level meter). Mean aerodynamic power (in W) was calculated by multiplying P_s in kPa by U in L/s. R_g was calculated by dividing P_s in kPa by U in L/s.

HSDI data were analyzed in MATLAB as follows. Video data from each experimental run were reviewed and two representative vibratory cycles were selected for further analysis. Next, individual frames, representing maximum glottal opening and closure, were selected for each vibratory cycle. The glottal midline and bilateral vocal fold medial edges were manually selected and traced for each frame. Distances in pixels were converted to metric units using a calibration algorithm and reference to a two-dimensional calibration grid employed during data collection (a single HSDI frame showing the calibration grid at the level of the glottis was recorded for each mounted larynx prior to initiating the first experimental run). Vibratory amplitude (in μm) and area (in μm^2) were then derived for both left and right vocal folds. Vibratory amplitude was measured midway between the anterior commissure and vocal process, and was defined as the change in distance from the vocal fold medial edge to the glottal midline, across maximum opening and closure frames. Vibratory area was defined as the change in area bordered by each unilateral vocal fold and the glottal midline, across maximum opening and closure frames. Inter- and intra-measurer agreement data were collected for 10% of experimental runs.

Statistical Analysis

P_{th} data were analyzed across experimental groups using a one-way analysis of variance (ANOVA). R_g and E_g data, collected at multiple P_s values for each larynx, were examined using longitudinal data analyses (LDAs), with experimental group, P_s and its square as fixed effects, and the intercept and squared P_s as larynx-specific random effects. Vibratory amplitude and vibratory area data were analyzed at P_{th} and 1.96 kPa using two-way ANOVAs, with experimental group and P_s as fixed effects, and their interaction term included. Inter- and intra-measurer agreement data were analyzed using the Bland- Altman procedure with limits of agreement set at 95% (Bland & Altman, 1986).

Logarithmic (base e) transformation of the P_{th}, R_g, E_g, vibratory amplitude and vibratory area data was performed a priori in order to better meet the equal variance assumptions of ANOVA and LDA. Inter- and intra-measurer agreement data were untransformed. In all ANOVA cases, if the omnibus F-test revealed significant differences, pairwise comparisons between experimental groups were examined (Fisher's protected least significant difference). An α-level of 0.05 was employed for all statistical testing. All *p*-values were two sided. All computations and figures were performed using R for Windows, version 2.4.1 patched (Feb 4th 2007) and SAS version 9.3 for Windows (SAS Institute, Cary, NC).

Results

Histology and Immunohistochemistry

Representative histological and IHC images of chronically scarred and control vocal folds are presented in Figure 4. All judges agreed that, compared with control, the lamina propria of the chronically scarred vocal folds was characterized by reduced HA abundance on Alcian blue stain, increased collagen abundance on Masson's trichrome stain, elevated collagen I abundance on IHC, and elevated collagen III abundance on IHC. In addition, all

judges commented that collagen III abundance was greater than collagen I abundance. Consensus was reached on all judgments. Agreement on repeat judgments was 100%.

Excised Larynx Phonation

Phonation was achieved and data were collected from all 6 control and 4 bFGF treated larynges. Phonation was not achieved at any P_s with 3 of the 6 chronically scarred and 1 of the 6 sham treated larynges.

Figure 5 contains P_{th} data across experimental groups. One-way ANOVA revealed a significant main effect (F [3, 14] = 5.86, p = .0083). Pairwise comparisons revealed significantly elevated P_{th} in the scar group compared with the control (p = .0364), sham (p = .0238) and bFGF (p = .0009) groups, and significantly reduced P_{th} in the bFGF group compared with the control group (p = .0306).

Figure 6 contains mean R_g and E_g data across experimental groups. LDA for R_g revealed no significant differences across groups. LDA for E_g revealed significantly reduced efficiency in the scar group compared with the control (p = .0416), sham (p = .0005) and bFGF (p = .0036) groups, and significantly increased efficiency in the sham group compared with the control group (p = .0105).

Vibratory amplitude and area data are presented in Figure 7 and Figure 8. Figure 7 contains example data from two larynges representative of the control and scar groups, collected from sequential experimental runs at P_s values below 4 kPa. The figure illustrates approximate superimposition of vibratory amplitude and area data from the left and right vocal folds in the control larynx, and consistently greater vibratory amplitude and area in the right (control) vocal fold compared with the left (scarred) vocal fold in the unilaterally scarred larynx.

Figure 8 illustrates experimental group differences in vibratory amplitude and area at P_{th} and 1.96 kPa. These data are expressed as a ratio of left versus right vocal fold, with a value of 1 representing symmetry. Two-way ANOVA for vibratory amplitude revealed a significant effect for experimental group (F [3, 27] = 6.00, p = .0029) and non-significant effects for P_s (F [1, 27] = 0.02, p = .9028) and the interaction term (F [3, 27] = 0.97, p = .4208). Pairwise comparisons for experimental group revealed significantly elevated ratios in the scar group compared with the control (p = .0084) and bFGF (p = .0010) groups, and a significantly elevated ratio in the sham group compared with the bFGF group (p = .0056). Two-way ANOVA for vibratory area revealed a significant effect for experimental group (F [3, 27] = 9.02, p = .0003) and non-significant effects for P_s (F [3, 27] = 0.54, p = .4685) and the interaction term (F [1, 27] = 0.22, p = .8843). Pairwise comparisons for experimental group revealed significantly elevated ratios in the scar group compared with the control (p = .0002), sham (p = .0135) and bFGF (p < .0001) groups, and a significantly elevated ratio in the sham group compared with the bFGF group (p = .0108).

Bland-Altman analyses of inter- and intra-measurer agreement data for the calculation of vibratory amplitude and area are summarized in Table 1. For vibratory amplitude, measurement bias was two-fold greater (1.26 μm) in the inter-measurer dataset compared with the intra-measurer dataset (0.63 μm); whereas for vibratory area, measurement bias was comparable across groups (-0.34×10^4 and -0.39×10^4 μm^2 respectively). The intra-measurer dataset was characterized by consistently narrower confidence intervals and limits of agreement compared with the inter-measurer dataset. Viewed across our entire dataset, these inter- and intra-measurer differences consistently represented < 2.5% variation in vibratory amplitude and < 5% variation in vibratory area.

Discussion

The purpose of this study was to develop and evaluate a rat excised larynx model for the measurement of acoustic, aerodynamic and vocal fold vibratory changes resulting from vocal fold scar. Chronically scarred vocal folds were characterized by elevated collagen I and III and reduced HA abundance compared with control. We successfully generated phonation data for unscarred larynges and bFGF treated scarred larynges, but were unable to achieve phonation in 3 of 6 scarred larynges and 1 of 6 sham treated larynges. Consistent with our hypotheses and data from other excised larynx models (Hirano, Bless, Nagai et al., 2004; Hirano, Bless, Rousseau et al., 2004; Rousseau, Montequin et al., 2004; Rousseau et al., 2006), the scar experimental group was characterized by elevated P_{th}, reduced E_g, and intra-larynx vibratory amplitude and area asymmetry, compared to control. The bFGF group was characterized by P_{th} below control group levels, E_g comparable to control, and vocal fold vibratory amplitude and area symmetry comparable to control. Unexpectedly, and counter to our hypotheses, the sham group was characterized by P_{th} comparable to control, E_g superior to control, and vocal fold vibratory amplitude and area symmetry comparable to control.

Histological/Immunohistochemical Findings

The increase in collagen I and III and decrease in HA abundance observed in the chronic scar group is consistent with data reported by Tateya et al. (2005). Tateya and colleagues observed peak collagen I abundance 2 weeks following vocal fold injury, followed by successive decreases in abundance at the 1 and 2 month time points. Collagen III abundance, in contrast, was consistently elevated at all time points from 2 weeks to 3 months. Consequently, chronically scarred vocal folds (2 months post injury and beyond) were characterized by relatively higher abundance of collagen III as opposed to collagen I. We observed a similar pattern in our chronic scar group where consensus judgment identified a slight increase in collagen I and greater increase in collagen III abundance, primarily in the superficial lamina propria.

It is important to note that we did not perform histology and IHC on the same larynges subjected to excised larynx phonation, due to concern that prolonged phonation at RT may result in tissue degradation that could compromise histological findings. Because of this however, we were unable to evaluate whether there were any distinct histological features that characterized the 4 larynges for which phonation was not achieved. Further, as these analyses were only performed on larynges in the chronic scar group for the purpose of confirming ECM alteration 2 months following injury creation, we did not confirm the successful delivery and uptake of bFGF in the scarred vocal fold, or investigate any cellular/extracellular features that might account for the favorable phonatory performance of larynges in the bFGF and sham treatment groups.

Improvement with bFGF Treatment

We observed clear improvement in phonatory function for chronically scarred vocal folds treated with a single 100 ng bFGF injection, demonstrating the sensitivity of this excised larynx model to treatment induced functional change. This finding is also supportive of a bFGF induced therapeutic benefit in scarred vocal folds that translates to improved biomechanical tissue performance, and aligns with previous work demonstrating that bFGF induces favorable changes in ECM protein synthesis by VFFs. Hirano and colleagues reported increased HA and decreased collagen I synthesis following bFGF administration to cultured canine and rat VFFs (Hirano, Bless, Muñoz del Río et al., 2004; Hirano et al., 2003), and elevated HA abundance with no change in collagen abundance in aged rat vocal folds, sustained for 2 months following 4 weekly 100 ng bFGF injections (Hirano et al.,

2005). HA is a key contributor to native vocal fold viscoelasticity (Chan, Gray, & Titze, 2001) and its depletion is characteristic of the scar phenotype (Rousseau et al., 2003; Tateya et al., 2005). Hence, the improvement in phonatory function observed following bFGF administration in this study may have resulted from the induction of new HA synthesis in resident fibroblasts. As the relationship between bFGF, HA synthesis, and biomechanical tissue change has not been directly examined in scarred vocal folds, this hypothesis requires additional testing.

Improvement with Sham Treatment

The improvement in phonatory function observed following sham treatment is provocative. Compared with control, the sham group demonstrated indistinguishable P_{th}, lower but non-significantly different R_g, and significantly elevated E_g. Vibratory amplitude and particularly area were more asymmetric in the sham group compared with control, but again this difference was non-significant. Interestingly, although comparable to control on the majority of indices, the sham group did not demonstrate the same magnitude of P_{th}, R_g and vibratory parameter improvement as observed for the bFGF group. Overall, these findings suggest either that saline injection alone is sufficient to realize biomechanical improvement in chronically scarred vocal folds (that remains inferior to that attainable with bFGF treatment), or that the dataset for this experimental group is artifactual. Published excised larynx scar experiments in larger animals that have included a saline sham condition have consistently reported sub-normal phonatory performance under this condition (Hirano, Nagai et al., 2004; Hirano, Rousseau et al., 2004). Whether the differences reported here are due to the size of the rat larynx, the presence of a tri-layered lamina propria that is not seen in other animals, or artifact, is unclear.

Variability and Limitations

The relatively high variability observed in the scar group dataset compared with the other experimental groups, alongside our inability to achieve phonation in 50% of chronically scarred larynges, may reflect phonatory instability inherent to vocal fold scar. Any such instability may have been amplified by the use of a unilateral scar model in this study, resulting in biomechanical differences between the left and right vocal folds and consequent aperiodic and potentially nonlinear output. Further, our inability to phonate a significant percentage of scarred larynges suggests that in certain cases the biomechanical tissue deficiency in the scarred vocal fold was too great to overcome at P_s values below 6 kPa. This biomechanical challenge is compounded by working with a membranous vocal fold length on the order of 1 mm and mucosal thickness on the order of 0.2 mm (Kurita et al., 1983). Several theoretical and modeling papers have described an inverse relationship between P_{th} and vocal fold length, thickness and overall size (Chan & Titze, 2006; Lucero & Koenig, 2005; Titze, 1988). Given this relationship, a scarred rat vocal fold will require significantly greater driving pressure to initiate and sustain phonation than a scarred vocal fold of equivalent viscosity in a larger animal. Stated otherwise, successful excised larynx phonation in profoundly scarred rat vocal folds might only be possible at extremely high P_s. This is a potential limitation of the rat model.

An additional source of potential variability in this study, which should influence all experimental conditions equally, stems from tissue specimen size and its relationship to measurement scale. Given the dimensions of the rat larynx, even slight variations in specimen mounting, suture placement, vocal fold tension and glottal aperture across experimental runs are likely to have a magnified influence on phonatory output, when compared with equivalent output generated using an excised larynx from a larger animal. This technical variability has the potential to influence all acoustic, aerodynamic and vocal fold vibratory measurements, but may be particularly important when considering the

micrometer scale of the distance measurements that underlie the vibratory amplitude and area calculations reported in this study. While we exercised stringent methodological care, the contribution of this source of variability to our findings (if any) is unknown.

Conclusions

This study represents the first report of successful excised larynx phonation in the rat. The excised larynx model described here demonstrated robust deterioration across aerodynamic, acoustic and vocal fold vibratory indices under the scar condition and sensitivity to treatment induced change under the bFGF condition. The improvement observed under the sham condition may reflect unanticipated therapeutic benefit or artifact. Future research should replicate and re-evaluate the sham treatment used here, focus on refinement of the technical challenges inherent in working with such small tissue specimens, and directly measure the relationship between the extent of scar induced ECM alteration and biomechanical performance. Additionally, the notable vibratory asymmetries observed under the unilateral chronic scar condition may be suited to characterization using non-linear techniques. Future work focused on bFGF should devote attention to timing and dosing variations, in addition to the specific cellular and extracellular functions of this growth factor in the vocal fold. This excised larynx model holds promise as a tool for the functional characterization of biomechanical tissue changes resulting from vocal fold ECM injury, and the evaluation of experimental therapies.

Acknowledgments

This study was supported by grant R01 DC004428 from the National Institute on Deafness and Other Communication Disorders. We acknowledge experimental setup consultation provided by Jack J. Jiang, M.D., Ph.D. and statistical consultation provided by Alejandro Muñoz del Río, Ph.D.

This study was performed in accordance with the PHS Policy on Humane Care and Use of Laboratory Animals, the NIH Guide for the Care and Use of Laboratory Animals, and the Animal Welfare Act (7 U.S.C. et seq.); the animal use protocol was approved by the Institutional Animal Care and Use Committee (IACUC) of the University of Wisconsin-Madison.

References

Akita S, Akino K, Tanaka K, Anraku K, Hirano A. A basic fibroblast growth factor improves lower extremity wound healing with a porcine-derived skin substitute. Journal of Trauma: Injury, Infection and Critical Care 2008;64:809–815.

Alipour F, Jaiswal S. Glottal airflow resistance in excised pig, sheep, and cow larynges. Journal of Voice. in press.

Alipour F, Jaiswal S, Finnegan E. Aerodynamic and acoustic effects of false vocal folds and epiglottis in excised larynx models. Annals of Otology, Rhinology and Laryngology 2007;116:135–144.

Alipour F, Scherer RC. On pressure-frequency relations in the excised larynx. Journal of the Acoustical Society of America 2007;122:2296–2305. [PubMed: 17902865]

Benninger MS, Alessi D, Archer S, Bastian R, Ford CN, Koufman J, et al. Vocal fold scarring: Current concepts and management. Otolaryngology—Head and Neck Surgery 1996;115:474–482. [PubMed: 8903451]

Berry DA, Reininger H, Alipour F, Bless DM, Ford CN. Influence of vocal fold scarring on phonation: Predictions from a finite element model. Annals of Otology, Rhinology and Laryngology 2005;114:847–852.

Bland JM, Altman DG. Statistical methods for assessing agreement between two methods of clinical measurement. Lancet 1986;327:307–310. [PubMed: 2868172]

Chan RW, Gray SD, Titze IR. The importance of hyaluronic acid in vocal fold biomechanics. Otolaryngology—Head and Neck Surgery 2001;124:607–614. [PubMed: 11391249]

Chan RW, Titze IR. Dependence of phonation threshold pressure on vocal tract acoustics and vocal fold tissue mechanics. Journal of the Acoustical Society of America 2006;119:2351–2362. [PubMed: 16642848]

Chhetri DK, Head C, Revazova E, Hart S, Bhuta S, Berke GS. Lamina propria replacement therapy with cultured autologous fibroblasts for vocal fold scars. Otolaryngology—Head and Neck Surgery 2004;131:864–870. [PubMed: 15577782]

Dailey SH, Tateya I, Montequin D, Welham N, Goodyer E. Viscoelastic measurements of vocal folds using the linear skin rheometer. Journal of Voice. in press.

Döllinger M, Berry DA. Visualization and quantification of the medial surface dynamics of an excised human vocal fold during phonation. Journal of Voice 2006a;20:401–413.

Döllinger M, Berry DA. Computation of the three-dimensional medial surface dynamics of the vocal folds. Journal of Biomechanics 2006b;39:369–374.

Döllinger M, Berry DA, Montequin DW. The influence of epilarynx area on vocal fold dynamics. Otolaryngology—Head and Neck Surgery 2006;135:724–729. [PubMed: 17071302]

Duflo S, Thibeault SL, Li W, Shu XZ, Prestwich GD. Vocal fold tissue repair in vivo using a synthetic extracellular matrix. Tissue Engineering 2006;12:2171–2180. [PubMed: 16968158]

Finnegan EM, Alipourx F. Phonatory effects of supraglottic structures in excised canine larynges. Journal of Voice. in press.

Gospodarowicz D. Localisation of a fibroblast growth factor and its effect alone and with hydrocortisone on 3T3 cell growth. Nature 1974;249:123–127. [PubMed: 4364816]

Gospodarowicz D. Purification of a fibroblast growth factor from bovine pituitary. Journal of Biological Chemistry 1975;250:2515–2520. [PubMed: 1168187]

Hansen JK, Thibeault SL, Walsh JF, Shu XZ, Prestwich GD. In vivo engineering of the vocal fold extracellular matrix with injectable hyaluronic acid hydrogels: Early effects on tissue repair and biomechanics in a rabbit model. Annals of Otology, Rhinology and Laryngology 2005;114:662–670.

Heldin P, Laurent TC, Heldin CH. Effect of growth factors on hyaluronan synthesis in cultured human fibroblasts. Biochemical Journal 1989;258:919–922. [PubMed: 2543365]

Hertegard S, Cedervall J, Svensson B, Forsberg K, Maurer FH, Vidovska D, et al. Viscoelastic and histologic properties in scarred rabbit vocal folds after mesenchymal stem cell injection. Laryngoscope 2006;116:1248–1254. [PubMed: 16826069]

Hirano S, Bless DM, Heisey D, Ford CN. Effect of growth factors on hyaluronan production by canine vocal fold fibroblasts. Annals of Otology, Rhinology and Laryngology 2003;112:617–624.

Hirano S, Bless DM, Muñz del Río A, Connor NP, Ford CN. Therapeutic potential of growth factors for aging voice. Laryngoscope 2004;114:2161–2167. [PubMed: 15564837]

Hirano S, Bless DM, Nagai H, Rousseau B, Welham NV, Montequin DW, et al. Growth factor therapy for vocal fold scarring in a canine model. Annals of Otology, Rhinology and Laryngology 2004;113:777–785.

Hirano S, Bless DM, Rousseau B, Welham NV, Montequin DW, Chan RW, et al. Prevention of vocal fold scarring by topical injection of hepatocyte growth factor in a rabbit model. Laryngoscope 2004;114:548–556. [PubMed: 15091233]

Hirano S, Nagai H, Tateya I, Tateya T, Ford CN, Bless DM. Regeneration of aged vocal folds with basic fibroblast growth factor in a rat model: A preliminary report. Annals of Otology, Rhinology and Laryngology 2005;114:304–308.

Jia X, Yeo Y, Clifton RJ, Jiao T, Kohane DS, Kobler JB, et al. Hyaluronic acid-based microgels and microgel networks for vocal fold regeneration. Biomacromolecules 2006;7:3336–3344. [PubMed: 17154461]

Jiang JJ, Zhang Y, Ford CN. Nonlinear dynamics of phonations in excised larynx experiments. Journal of the Acoustical Society of America 2003;114:2198–2205. [PubMed: 14587617]

Jiang JJ, Zhang Y, Stern J. Modeling of chaotic vibrations in symmetric vocal folds. Journal of the Acoustical Society of America 2001;110:2120–2128. [PubMed: 11681389]

Kanemaru S, Nakamura T, Omori K, Kojima H, Magrufov A, Hiratsuka Y, et al. Regeneration of the vocal fold using autologous mesenchymal stem cells. Annals of Otology, Rhinology and Laryngology 2003;112:915–920.

Khosla S, Murugappan S, Gutmark E, Scherer R. Vortical flow field during phonation in an excised canine larynx model. Annals of Otology, Rhinology and Laryngology 2007;116:217–228.

Khosla S, Murugappan S, Lakhamraju R, Gutmark E. Using particle imaging velocimetry to measure anterior-posterior velocity gradients in the excised canine larynx model. Annals of Otology, Rhinology and Laryngology 2008;117:134–144.

Krishna P, Rosen CA, Branski RC, Wells A, Hebda PA. Primed fibroblasts and exogenous decorin: Potential treatments for subacute vocal fold scar. Otolaryngology—Head and Neck Surgery 2006;135:937–945. [PubMed: 17141088]

Kurita, S.; Nagata, K.; Hirano, M. A comparative study of the layer structure of the vocal fold. In: Bless, DM.; Abbs, JH., editors. Vocal fold physiology: Contemporary research and clinical issues. San Diego: College-Hill Press; 1983. p. 3-21.

Lucero JC, Koenig LL. Phonation thresholds as a function of laryngeal size in a two-mass model of the vocal folds. Journal of the Acoustical Society of America 2005;118:2798–2801. [PubMed: 16334896]

Luo Y, Kobler JB, Zeitels SM, Langer R. Effects of growth factors on extracellular matrix production by vocal fold fibroblasts in 3-dimensional culture. Tissue Engineering 2006;12:3365–3374. [PubMed: 17518673]

Ohno T, Hirano S, Kanemaru S, Yamashita M, Umeda H, Suehiro A. Drug delivery system of hepatocyte growth factor for the treatment of vocal fold scarring in a canine model. Annals of Otology, Rhinology and Laryngology 2007;116:762–769.

Ono I, Akasaka Y, Kikuchi R, Sakemoto A, Kamiya T, Yamashita T, et al. Basic fibroblast growth factor reduces scar formation in acute incisional wounds. Wound Repair and Regeneration 2007;15:617–623. [PubMed: 17971006]

Ornitz DM, Itoh N. Fibroblast growth factors. Genome Biology 2001;2 Reviews 3005.1-3005.12.

Palmon A, Roos H, Edel J, Zax B, Savion N, Grosskop A, et al. Inverse dose- and time-dependent effect of basic fibroblast growth factor on the gene expression of collagen type I and matrix metalloproteinase-1 by periodontal ligament cells in culture. Journal of Periodontology 2000;71:974–980. [PubMed: 10914801]

Palmon A, Roos H, Reichenberg E, Grosskop A, Bar Kana I, Pitaru S, et al. Basic fibroblast growth factor suppresses tropoelastin gene expression in cultured human periodontal fibroblasts. Journal of Periodontal Research 2001;36:65–70. [PubMed: 11327080]

Petersen G, Johnson P, Andersson L, Klinga-Levan K, Gomez-Fabre PM, Stahl F. RatMap—rat genome tools and data. Nucleic Acids Research 2005;33:D492–D494. [PubMed: 15608244]

Rapraeger AC, Krufka A, Olwin BB. Requirement of heparan sulfate for bFGF-mediated fibroblast growth and myoblast differentiation. Science 1991;252:1705–1708. [PubMed: 1646484]

Rousseau B, Hirano S, Chan RW, Welham NV, Thibeault SL, Ford CN, et al. Characterization of chronic vocal fold scarring in a rabbit model. Journal of Voice 2004;18:116–124. [PubMed: 15070231]

Rousseau B, Hirano S, Scheidt TD, Welham NV, Thibeault SL, Chan RW, et al. Characterization of vocal fold scarring in a canine model. Laryngoscope 2003;113:620–627. [PubMed: 12671417]

Rousseau B, Montequin DW, Tateya I, Bless DM. Functional outcomes of reduced hyaluronan in acute vocal fold scar. Annals of Otology, Rhinology and Laryngology 2004;113:767–776.

Rousseau B, Tateya I, Lim X, Muñoz del Río A, Bless DM. Investigation of anti-hyaluronidase treatment on vocal fold wound healing. Journal of Voice 2006;20:443–451. [PubMed: 16243482]

Tateya T, Tateya I, Sohn JH, Bless DM. Histologic characterization of rat vocal fold scarring. Annals of Otology, Rhinology and Laryngology 2005;114:183–191.

Thibeault SL, Gray SD, Bless DM, Chan RW, Ford CN. Histologic and rheologic characterization of vocal fold scarring. Journal of Voice 2002;16:96–104. [PubMed: 12002893]

Titze IR. The physics of small-amplitude oscillation of the vocal folds. Journal of the Acoustical Society of America 1988;83:1536–1552. [PubMed: 3372869]

Titze IR. On the relation between subglottal pressure and fundamental frequency in phonation. Journal of the Acoustical Society of America 1989;85:901–906. [PubMed: 2926005]

van den Berg JW. Vocal ligaments versus registers. Current Problems in Phoniatrics and Logopedics 1960;1:19–34.

van den Berg JW, Tan TS. Results of experiments with human larynxes. Practica Oto-Rhino-Laryngologica 1959;21:425–450. [PubMed: 13841006]

Xu CC, Chan RW, Tirunagari N. A biodegradable, acellular xenogeneic scaffold for regeneration of the vocal fold lamina propria. Tissue Engineering 2007;13:551–566. [PubMed: 17518602]

Yayon A, Klagsbrun M, Esko JD, Leder P, Ornitz DM. Cell surface, heparin-like molecules are required for binding of basic fibroblast growth factor to its high affinity receptor. Cell 1991;64:841–848. [PubMed: 1847668]

Zhang Y, Jiang JJ, Tao C, Bieging E, MacCallum JK. Quantifying the complexity of excised larynx vibrations from high-speed imaging using spatiotemporal and nonlinear dynamic analyses. Chaos 2007;17 043114.

Zhao W, Han Q, Lin H, Gao Y, Sun W, Zhao Y, et al. Improved neovascularization and wound repair by targeting human basic fibroblast growth factor (bFGF) to fibrin. Journal of Molecular Medicine. in press.

Zittermann SI, Issekutz AC. Basic fibroblast growth factor (bFGF, FGF-2) potentiates leukocyte recruitment to inflammation by enhancing endothelial adhesion molecule expression. American Journal of Pathology 2006a;168:835–846. [PubMed: 16507899]

Zittermann SI, Issekutz AC. Endothelial growth factors VEGF and bFGF differentially enhance monocyte and neutrophil recruitment to inflammation. Journal of Leukocyte Biology 2006b; 80:247–257. [PubMed: 16818728]

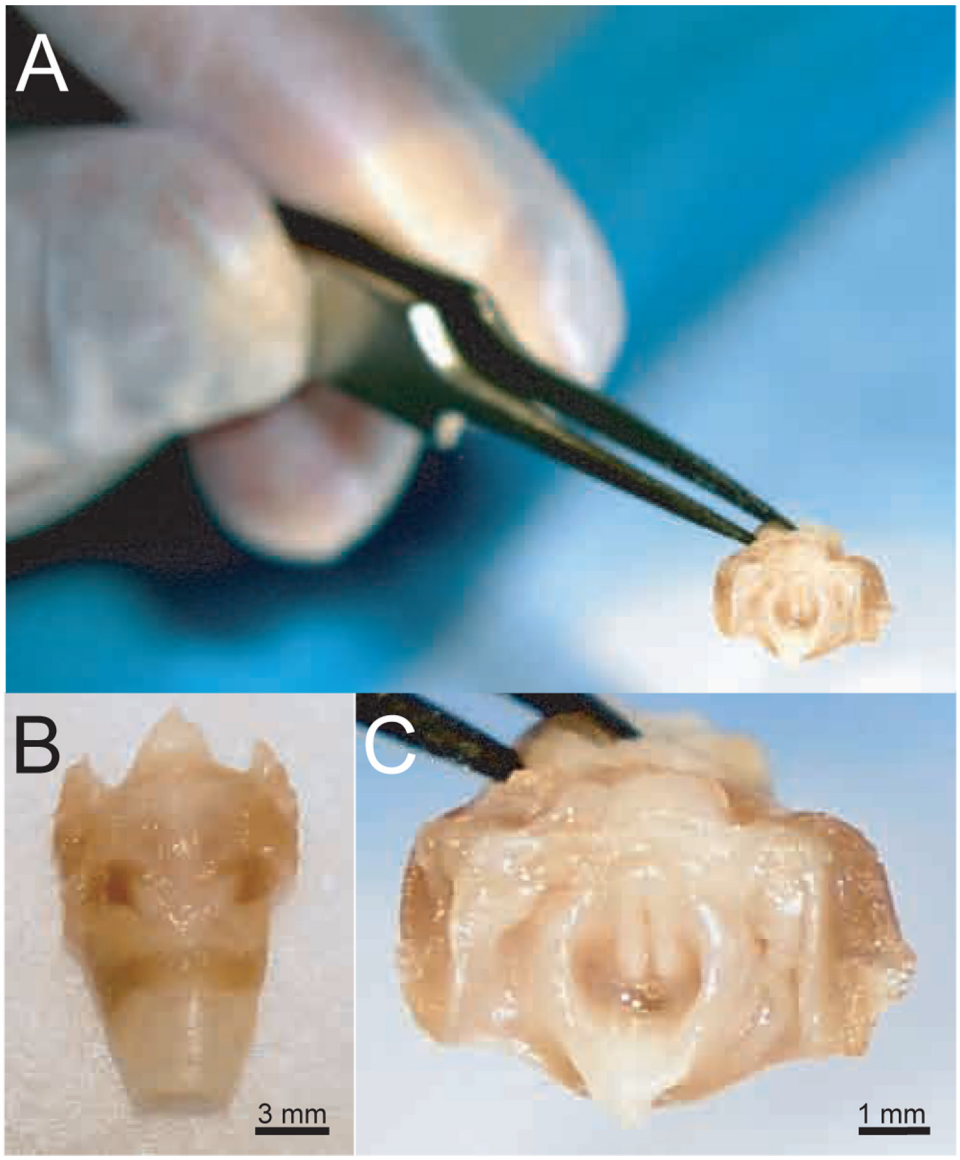

Figure 1.
Scale photographs of a rat excised larynx. A: Superior view, relative to human fingers. B: Magnified anterior view. C: Magnified superior view.

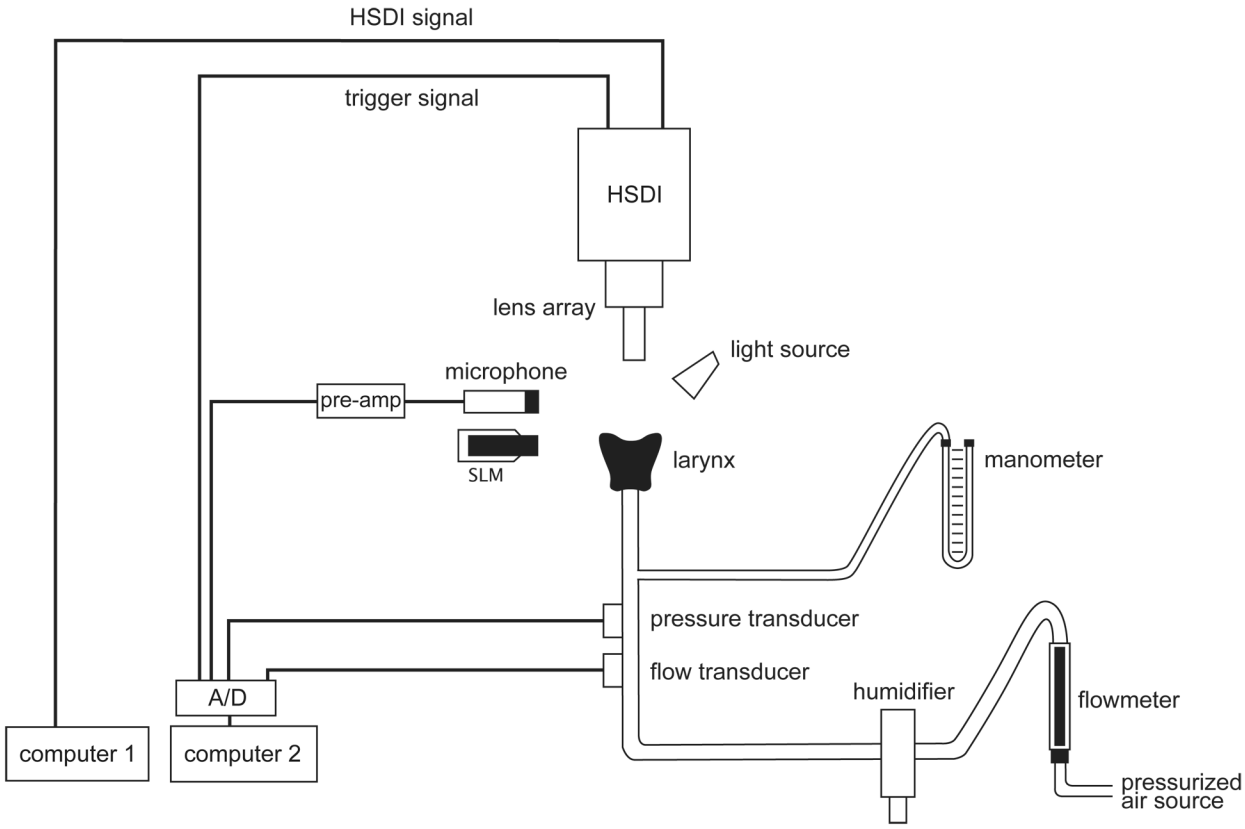

Figure 2.
Schematic of the excised larynx setup used in this experiment.

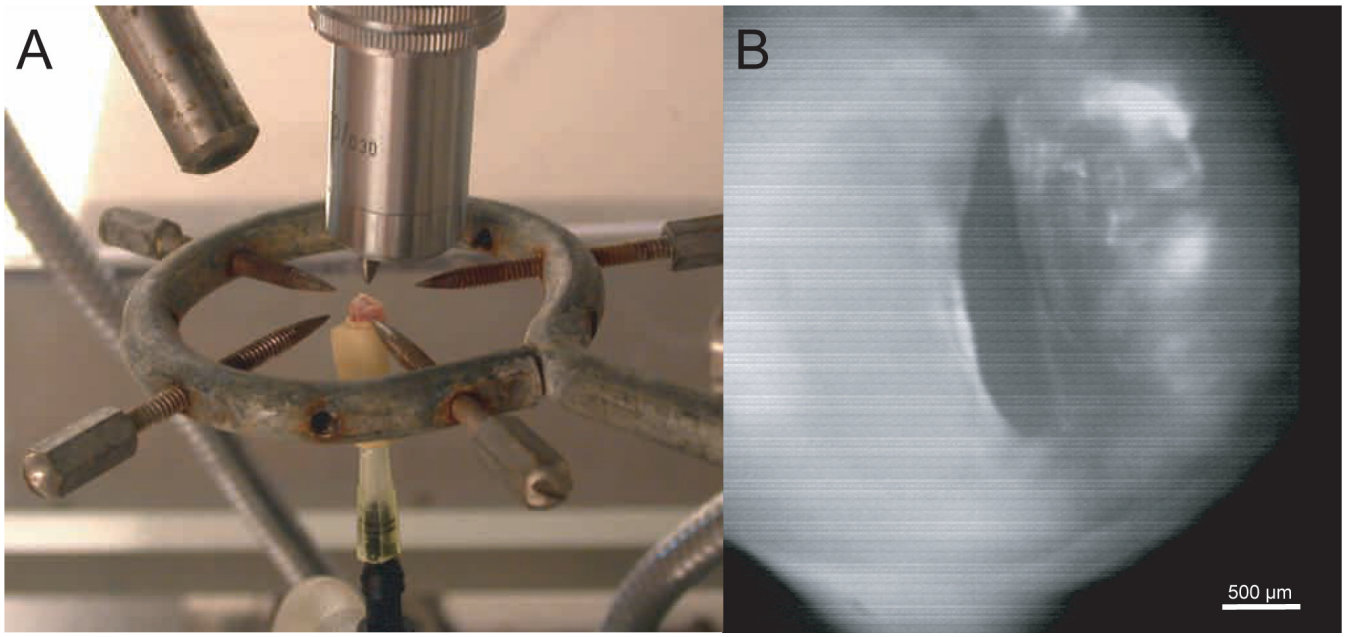

Figure 3.
A: Photograph of a mounted rat excised larynx. B: HSDI of the glottis during excised larynx phonation, taken from a larynx with unilateral chronic scar.

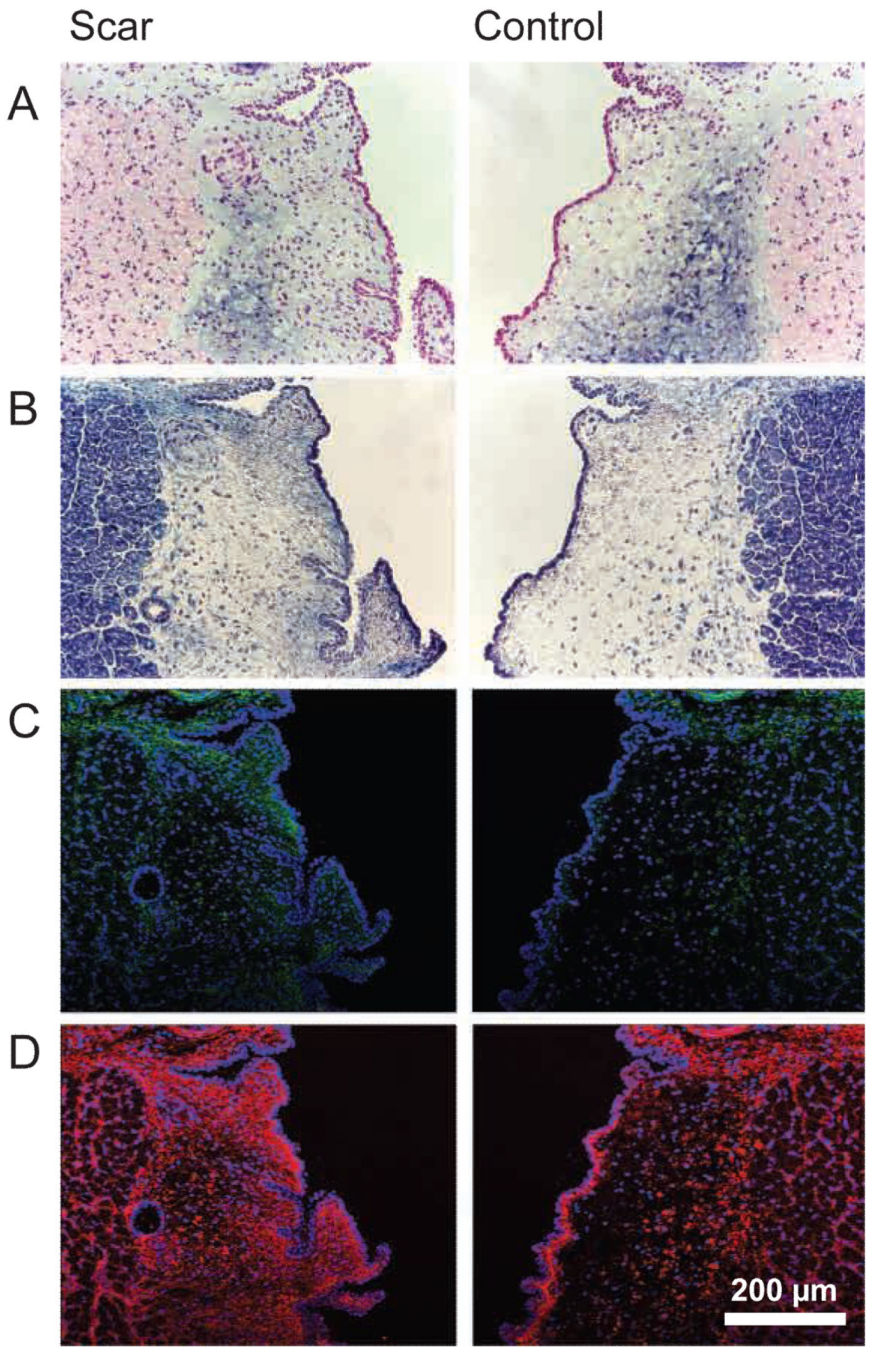

Figure 4.
Representative histological and immunohistochemical images of chronically scarred and control vocal folds. A: Alcian blue stain for HA. HA is stained blue and its presence was confirmed using a hyaluronidase digestion control (see text). B: Masson's trichrome stain. Collagen is stained blue. C: Collagen I immunostain. Collagen I is green; cell nuclei are blue. D: Collagen III immunostain. Collagen III is red; cell nuclei are blue.

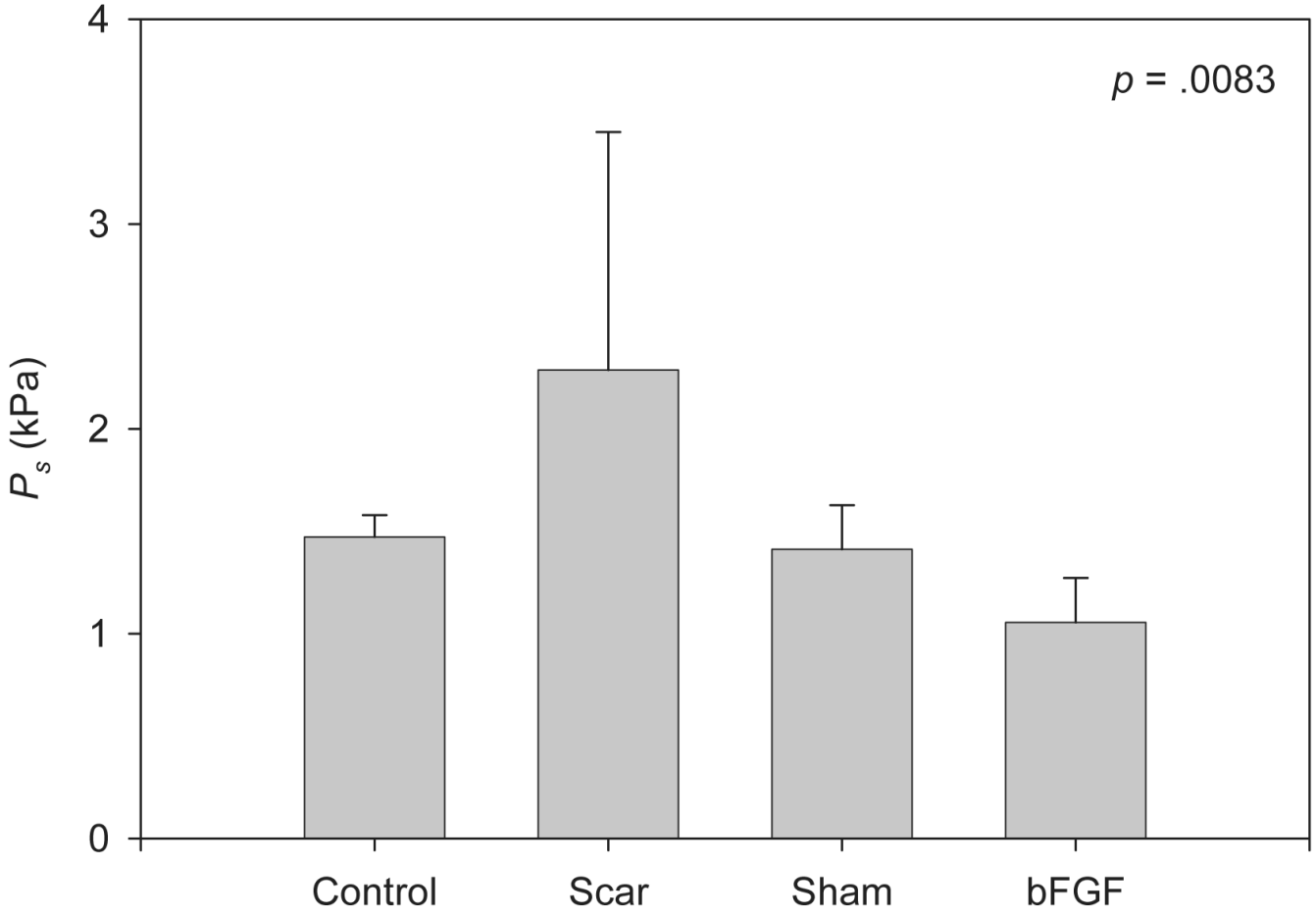

Figure 5.
P_{th} data across experimental groups. The *p*-value reflects a one-way ANOVA, which was performed on natural logarithm transformed data.

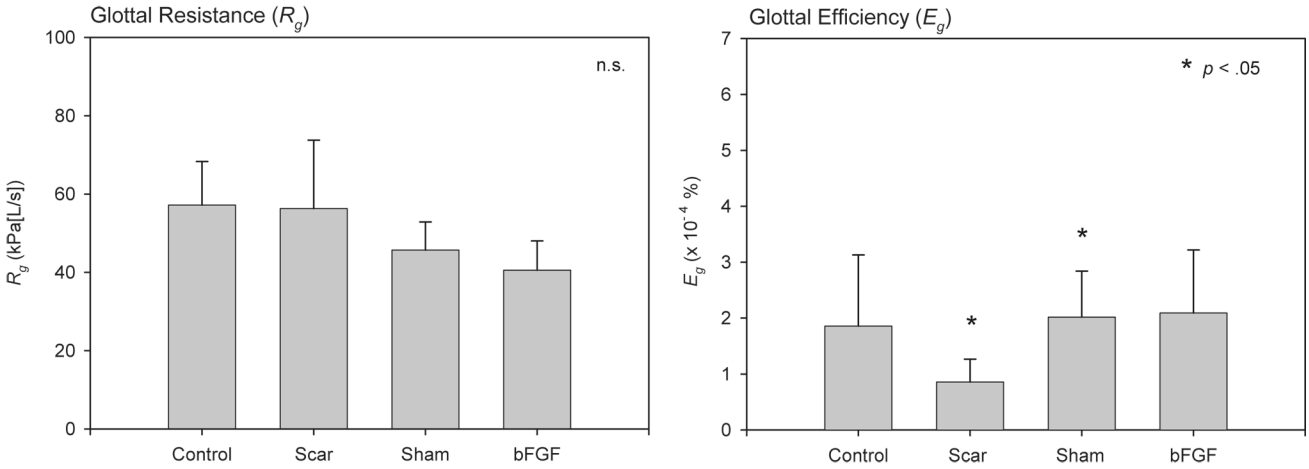

Figure 6.
Mean R_g and E_g data across experimental groups. The *p*-values reflect LDA based comparisons of the control condition against the other experimental conditions, which were performed on natural logarithm transformed data. Additional statistically significant comparisons are reported in the text.

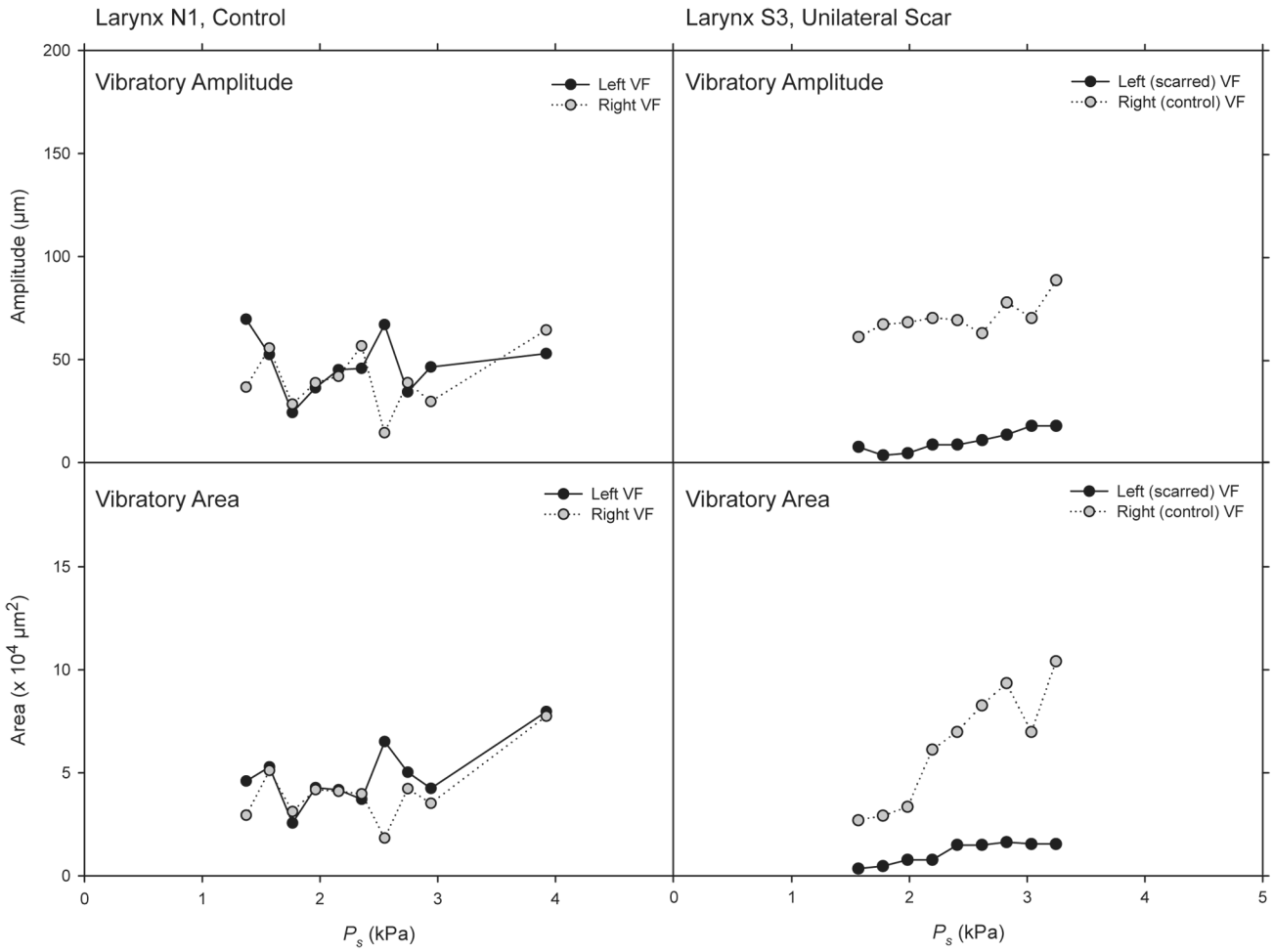

Figure 7.
Vibratory amplitude and area data from two larynges representative of the control and scar groups, collected from sequential experimental runs at P_s values below 4 kPa.

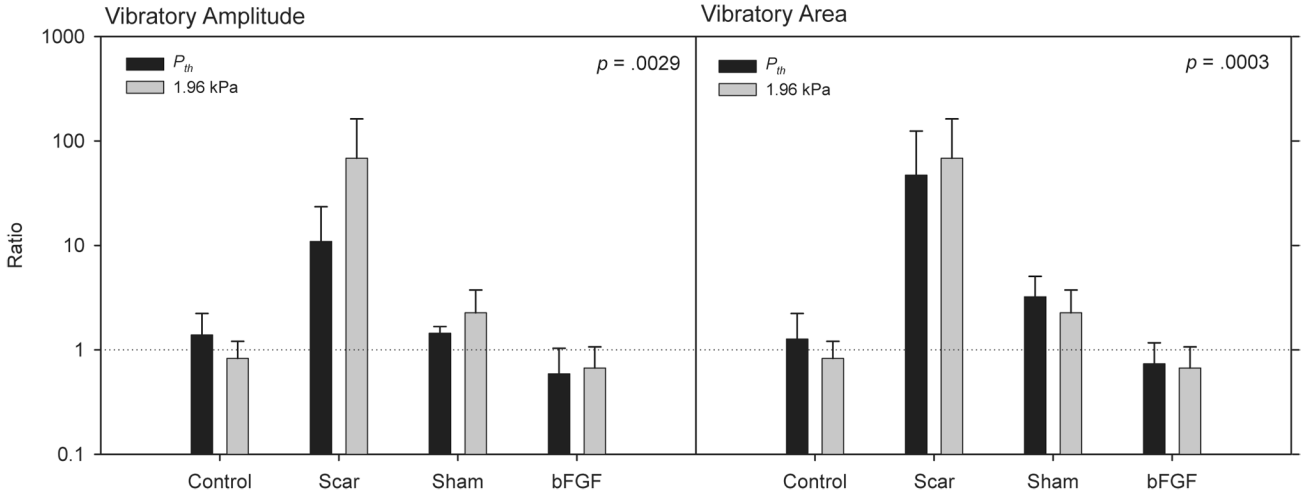

Figure 8.
Vibratory amplitude and area data measured at P_{th} and 1.96 kPa. Data are expressed as a ratio of left versus right vocal fold, with a value of 1 representing symmetry. The *p*-values reflect the ANOVA fixed effect for experimental group. ANOVAs were performed on natural logarithm transformed data.

Table 1

Bland-Altman analysis of inter- and intra-measurer agreement data.

	Bias (95% CI)	Lower Limit of Agreement	Upper Limit of Agreement
Vibratory amplitude (μm)			
Inter-measurer	1.26 (−6.34 – 8.88)	−45.98	48.52
Intra-measurer	0.63 (−3.17 – 4.44)	−23.00	24.26
Vibratory Area (×10^4 μm^2)			
Inter-measurer	−0.34 (−5.07 — 1.72)	−12.04	5.25
Intra-measurer	−0.39 (−1.59 — 0.80)	−7.81	7.03

Note. Limits of agreement were set at 95%. CI: Confidence Interval.